A greener pathway to enantiopurity: mechanochemical deracemization through abrasive grinding.

Chrystal LOPES[a,b], Yohann CARTIGNY[b], Clément BRANDEL[b], Oleksii SHEMCHUK[a], Tom LEYSSENS*[a]

[a] C. Lopes, Dr. O. Shemchuk, Prof. Dr. T. Leyssens
Department of Molecular Chemistry, Materials and Catalysis
Institute of Condensed Matter and Nanosciences
Université Catholique de Louvain
Place Louis Pasteur, 1 bte L4.01.06BE-1348 Louvain-La-Neuve (Belgium)
Tom.leyssens@uclouvain.be

[b] Dr. Y. Cartigny, Dr. C. Brandel
Département Chimie
Laboratoire Sciences et Méthodes Séparatives
Université Rouen Normandie
Place Emile Blondel, 76130 Mont-Saint-Aignan (France)

Supporting information for this article is given via a link at the end of the document.

Abstract: *We report the first case of mechanochemical deracemization. The target molecule is a precursor of Paclobutrazol, an important fungicide and plant growth inhibitor. Using mechanochemical deracemization enantiopurity can be reached much more rapidly compared to a solution based deracemization methodology. The present paper introduces an efficient and greener process to enantiopure material.*

Homochirality is an intrinsic property of life.[1] Biological systems are therefore often sensitive to stereochemistry,[2] with the two enantiomers of an active compound potentially presenting significant differences in pharmacological properties[3].

In 2005[4], Viedma reported the total conversion of a racemic mixture into a homochiral solid by continuous stirring and attrition of the racemic crystal suspension in equilibrium with a saturated solution. This process relies on a complex interplay between solution racemization and crystal ripening which amplifies imbalances between the different enantiomeric crystal populations. Latter coined “Viedma Ripening” (VR, hereafter) or more generally “deracemization by abrasive grinding”, the process permits to reach a total enantiomeric conversion of the solid state. It is however limited to conglomerate forming compounds[5] (both enantiomers crystallize in different crystals), which are furthermore characterized by rapid racemization in solution (usually involving the use of a racemizing agent)[6]. VR has been successfully applied to deracemize a multitude of racemic mixtures, including inorganic compounds, as well as small organic molecules[7,8], and several variants of this technique have been since developed[9–11].

Plant Growth inhibitors are widely used in the field of agro-chemistry. One such inhibitor, paclobutrazol (PBZ), also known as (2R,3R; 2S,3S)-1-(4-chloro-phenyl) 4,4-dimethyl-2-(1,2,4-triazol-1-yl)-pentan-3-ol[12] is sold as a racemic mixture, even though both enantiomers have distinct biological properties.[13] Whereas the (2R, 3R) enantiomer is mainly responsible for the antifungal activity, the (2S, 3S) enantiomer has regulation and inhibiting properties[14]. PBZ can be synthesized from 1-(4-chlorophenyl)-4,4-dimethyl-2-(1,2,4-triazol-1-yl)pentan-3-one (Compound 1 hereafter), which crystallizes as a conglomerate and which can undergo rapid solution racemization via a keto-enol equilibrium (Figure 1). Compound 1 has been successfully deracemized Temperature Cycle Induced Deracemization (TCID) processes.[15–17] This procedure can easily be reproduced (Fig. 2), and is characterized by a long induction period (4.2 days), lengthily overall process time (± 7 days), and showing an autocatalytic behavior all characteristic of the solution-based VR process. Beside the lengthily process times, solution-based deracemization processes require substantial amounts of solvent, often organic solvents, to allow for racemization.

To tackle both issues, we aimed at transposing the deracemization process to a concentrated solvent-free environment. To do so, we focused on the emerging field of mechanochemistry, considering its recent successes in performing organic reactions in a solvent-free manner. [18–20] Furthermore, Ikekawa and Haykawa [21] showed how racemization can successfully be achieved mechanochemically working on L-Leucine.

Figure 1. Keto-enol equilibrium of compound 1.

We here successfully introduce a solvent-free mechanochemical VR process, showing a significant reduction of the process time. Deracemization of compound 1 is achieved using high energy milling and a mere catalytic amount of solvent (Liquid Assisted Grinding, LAG). This is the first reported full “solid-state deracemization” based on the VR methodology paving the way for the development of ‘greener’ deracemization methodologies.

In an initial set of exploratory trial, we started from the racemate using sodium hydroxide (NaOH) as racemizing agent similar to the solution-based VR procedure.[17] Water-LAG was performed with a mixer-mill equipped with zirconium oxide vessels. These latter were charged with 100mg of racemate (*ee*=0%), 0.033g of NaOH (2.5 eq) and 10µL of water. The small amount of water added, allows for creation of sufficient amount of amorphous phase in which racemization occurs. For two of the six eperiments (Table S5) the *ee* shifted from 0% up to 60%, showing for the first time the feasibility of a solvent-free mechanochemical deracemization process. As for solution-based processes random emergence of a chiral end-state occurs. The 4 processes not showing substantial deracemization likely remained in an induction period similar to the induction period observed for solution-based processes. Remarkably, those process leading to 60% *ee* do so in an incredibly short process time of 4 to 7h.

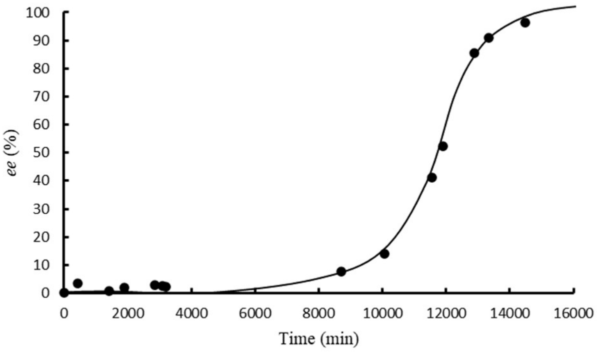

Figure 2. Deracemization of compound (±)-1 using classic Viedma Ripening in a TCID process.

In the solvent-based approach induction times are attributed to the lack of an initial crystal population imbalance when starting with a racemate. To circumvent this, the process can be started introducing an initial *ee*, placing the system in the exponential part of the kinetic curve. We took a similar intake for further experiments, starting with an initial 10%*ee* in an attempt to monitor the deracemization kinetics. To gain information on the process kinetics, and as homogeneous sampling during milling was not feasible with our set-up, the experiment was repeated numerous times, for an overall of 42 experiments, varying the process time for each (Table S6). Interestingly, the data seems to indicate that even starting with an intial *ee* of 10% there is still an induction time of about 30 minutes (MM-10-1 to MM-10-8). This in contrast to solution-based VR process which start from an initial population imbalance and do no longer show such an induction period. This induction period, typical to the mechanochemical process, is believed by us to be due to the necessity for the creation of a racemization media, which is here expected to be an amorphous phase containing the compound of interest, the small amount of water and some dissolved base. Such activation periods are commonly encountered in mechanochemical organic reaction processes.[22–24]

Following this initial induction, deracemization rapidly sets in, as shown by samples MM-1-9 to MM-1-42. After a mere 3h reaction time, *ee*s varying from 77 to 97% are obtained, highlighting the tremendous kinetic advantage of mechanochemical deracemization with respect to solution based deracemization (as a comparison, Fig. 2 shows the transformation from 10% *ee* to full deracemization to still take about 120h for the solution-based process). Mechanochemical deracemization also shows strong variation between experiments having identical reaction time. This cannot only be explained by the above-mentioned stochastic induction time as even after 180 min (end of the process), this variation remains. This can in part be explained by the ratio of amorphous vs crystalline phase. This former is the medium in which rapid racemization occurs and which therefore contains a near-racemic composition. For the analysis of our samples both amorphous and crystalline phase are recovered.[1] As the ratio of amorphous vs crystalline phase is expected to vary from one experiment to the other, so is the overall *ee*. For future process optimization, parameters impacting the amount of amorphous vs. crystalline phase will need to be carefully controlled, to achieve the highest *ee* possible.

Figure 3 graphically illustrates the data points of Table 6, with each data point belonging to a different autocatalytic kinetic curve. As a guide to the eye, some of these curves are drawn, to highlight the origin of the strong variation observed in mechanochemical deracemization. Interestingly, the spread in Figure 3, does show (i) a deracemization kinetics following the autocatalytic behavior, also encountered during the solution-based VR processes (ii) deracemization to be achieved in time-spans incredibly quicker compared to the solution-based processes. The blue dotted line in Figure 3 represents the shortest induction time possible for the reaction to set in and corresponds to time needed to create an amorphous phase in which racemization occurs. This induction period is likely impacted by mechanochemical conditions such as the amount of water, number of grinding beads, amount of beads vs material, …. The red dotted line, represents the underlying stochastic variability in induction time. Finally, the purple dotted line represents the spread in final *ee* likely due to the proportion of amorphous vs crystalline phase at the end of the experiment. In an ideal set-up, this spread should be kept as narrow as possible with an average value close to 100% *ee*. In a solution-based process, the racemate remaining in solution at the end of the process is removed by filtration, whereas in a mechanochemical process separation of the amorphous from crystalline phase cannot be performed, explaining the overall 80% *ee* measured at the end of the process. To achieve the highest enantiopurity possible, the amount of amorphous material present during the final stages of the grinding process should therefore be reduced as much as possible (eg. reducing the grinding spread at the end of the process, reducing the temperature at the end of the process, …).

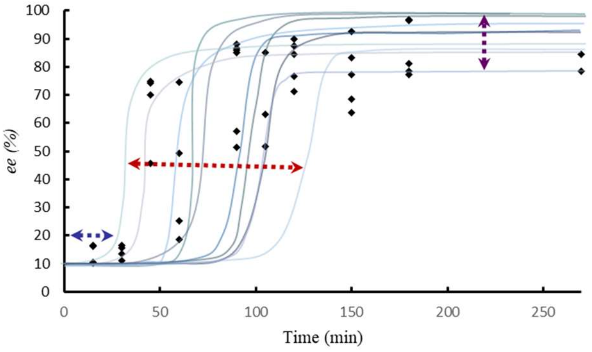

Figure 3. Deracemization kinetics of compound 1 under high energy milling conditions.

In this paper, we introduce a greener pathway to enantiopurity, being the first to enable viedma ripening mechanochemically. Even though a full mechanistic understanding is not yet achieved, results indicate that high energy milling yields enantioenriched material in a process much faster than the classic solution-based processes. Although some characteristics of the solution-based process (autocatalytic kinetics, induction time to population imbalance) are also encountered here, our data suggests careful control of amorphous vs crystalline phase is going to be key to truly understanding and optimizing these processes.

Acknowledgements

The authors from Normandie Université thank the Graduate School of Research XL-Chem (ANR-18-EURE-0020 XL-Chem) and the Région Normandie for financial support.

---

[1] This corresponds to recovering the racemic solution together with the enantiopure solid in a classical suspension based VR process.

Keywords: Deracemization, mechanochemistry, enantiomers, Viedma Ripening

[1] N. M. Maier, P. Franco, W. Lindner, *Journal of Chromatography A* **2001**, *906*, 3–33.

[2] M. Lämmerhofer, *Journal of Chromatography A* **2010**, *1217*, 814–856.

[3] R. Xie, L.-Y. Chu, J.-G. Deng, *Chemical Society Reviews* **2008**, *37*, 1243–1263.

[4] C. Viedma, *Phys. Rev. Lett.* **2005**, *94*, 065504.

[5] S. N. Black, L. J. Williams, R. J. Davey, F. Moffatt, D. M. McEwan, D. E. Sadler, R. Docherty, D. J. Williams, *J. Phys. Chem.* **1990**, *94*, 3223–3226.

[6] S. N. Black, L. J. Williams, R. J. Davey, F. Moffatt, R. V. H. Jones, D. M. McEwan, D. E. Sadler, *Tetrahedron* **1989**, *45*, 2677–2682.

[7] W. L. Noorduin, B. Kaptein, H. Meekes, W. J. P. van Enckevort, R. M. Kellogg, E. Vlieg, *Angew. Chem.* **2009**, *121*, 4651–4653.

[8] L.-C. Sögütoglu, R. R. E. Steendam, H. Meekes, E. Vlieg, F. P. J. T. Rutjes, *Chemical Society Reviews* **2015**, *44*, 6723–6732.

[9] F. Cameli, C. Xiouras, G. D. Stefanidis, *CrystEngComm* **2018**, *20*, 2897–2901.

[10] K. Intaraboonrod, T. Lerdwiriyanupap, M. Hoquante, G. Coquerel, A. E. Flood, *Mendeleev Communications* **2020**, *30*, 395–405.

[11] G. Belletti, C. Tortora, I. D. Mellema, P. Tinnemans, H. Meekes, F. P. J. T. Rutjes, S. B. Tsogoeva, E. Vlieg, *Chemistry – A European Journal* **2020**, *26*, 839–844.

[12] P. R. Soumya, P. Kumar, M. Pal, *Ind J Plant Physiol.* **2017**, *22*, 267–278.

[13] H.-M. Guo, Y. Zhao, M.-N. O. Yang, Z.-H. Yang, J.-H. Li, *Journal of Hazardous Materials* **2020**, *386*, 121882.

[14] T. D. Davis, E. A. Curry, G. L. Steffens, *Critical Reviews in Plant Sciences* **1991**, *10*, 151–188.

[15] G. Levilain, C. Rougeot, F. Guillen, J.-C. Plaquevent, G. Coquerel, *Tetrahedron: Asymmetry* **2009**, *20*, 2769–2771.

[16] K. Suwannasang, A. E. Flood, C. Rougeot, G. Coquerel, *Crystal Growth & Design* **2013**, *13*, 3498–3504.

[17] C. Rougeot, F. Guillen, J.-C. Plaquevent, G. Coquerel, *Crystal Growth & Design* **2015**, *15*, 2151–2155.

[18] T. Friščić, C. Mottillo, H. M. Titi, *Angewandte Chemie* **2020**, *132*, 1030–1041.

[19] J. Andersen, J. Mack, *Green Chem.* **2018**, *20*, 1435–1443.

[20] E. Colacino, F. Delogu, T. Hanusa, *ACS Sustainable Chem. Eng.* **2021**, *9*, 10662–10663.

[21] A. Ikekawa, S. Hayakawa, *Bulletin of the Chemical Society of Japan* **1984**, *57*, 889–890.

[22] H. Kulla, S. Haferkamp, I. Akhmetova, M. Röllig, C. Maierhofer, K. Rademann, F. Emmerling, *Angewandte Chemie International Edition* **2018**, *57*, 5930–5933.

[23] S. Haferkamp, F. Fischer, W. Kraus, F. Emmerling, *Beilstein J. Org. Chem.* **2017**, *13*, 2010–2014.

[24] H. Kulla, M. Wilke, F. Fischer, M. Röllig, C. Maierhofer, F. Emmerling, *Chem. Commun.* **2017**, *53*, 1664–1667.

Entry for the Table of Contents

((Insert graphic for Table of Contents here (300 DPI resolution: up to 650x532 pixels for single-column format; up to 1358x295 pixels for double-column format). Please ensure your graphic is in **one** of the two following formats))

((max. width: 5.5 cm; max. height: 4.5 cm))
650x532 pixels
Please delete this box prior to submission

or

((max. width: 11.0 cm; max. height: 2.5 cm))
1358x295 pixels
Please delete this box prior to submission

Insert text for Table of Contents here. ((maximum 450 characters including spaces; please provide a Table of Contents text that gives readers a short preview of the main theme of the research and results included in the paper to attract their attention into reading the paper in full. Define acronyms, including those in the picture! The Table of Contents text should be different from the abstract))

Institute and/or researcher Twitter usernames: ((optional))